Journal of Organometallic Chemistry, 312 (1986) 81–95
Elsevier Sequoia S.A., Lausanne – Printed in The Netherlands

ELECTROCHEMICALLY-INDUCED ISOMERIZATION OF $\{(\eta^5\text{-}C_5H_5)Mo(CO)_2(\mu\text{-}SR)\}_2$ (R = Me, t-Bu, Ph) COMPLEXES. ^{1}H NMR AND ELECTROCHEMICAL STUDIES. SYNTHESIS AND X-RAY CRYSTAL STRUCTURE OF $\{(\eta^5\text{-}C_5H_5)Mo(CO)_2(\mu\text{-}S\text{-}t\text{-}Bu)\}_2(BF_4)_2$

J. COURTOT-COUPEZ, M. GUÉGUEN, J.E. GUERCHAIS, F.Y. PÉTILLON *, J. TALARMIN *

Laboratoire de Chimie, Electrochimie et Photochimie Moléculaires, Faculté des Sciences et Techniques, Université de Bretagne Occidentale, 29287 Brest-Cedex (France)

and R. MERCIER

Laboratoire d'Electrochimie des Solides, Associé au C.N.R.S. No. 436, Faculté des Sciences, Université de Franche-Comté, 25030 Besançon-Cedex (France)

(Received March 25th, 1986)

Summary

The first example of geometrical isomerization of thiolato-bridged dimolybdenum complexes induced by the transfer of two electrons at the same potential is reported. Variable temperature ^{1}H NMR (R = Me, Ph) studies and an X-ray crystal structure determination for the dication (R = t-Bu) allowed the isomers to be identified. Comparisons of the cyclic voltammetry of the compounds $\{(\eta^5\text{-}C_5H_5)Mo(CO)_2(\mu\text{-}SR)\}_2$ (R = Me, t-Bu, Ph) suggest that steric factors are responsible for the preferred *trans* geometry of the neutral complexes.

The compound $\{(\eta^5\text{-}C_5H_5)(CO)_2\overline{Mo(\mu\text{-}S\text{-}t\text{-}Bu)_2}\overline{Mo}(CO)_2(\eta^5\text{-}C_5H_5)\}(BF_4)_2 \cdot CH_3CN$ has been characterized by X-ray diffraction. The crystals are orthorhombic, space group $P2_12_12_1$, with four molecules in a unit cell of dimensions *a* 10.598(3), *b* 13.489(3), *c* 21.801(3) Å. The structure was refined to $R = 0.60$.

The presence of Mo–S bonds in a variety of redox enzymes [1] has prompted synthetic [1,2] and electrochemical [3–6] studies of sulfur-containing complexes. In the course of a study of this type of compounds, we observed that the oxidative electrochemistry of the $\{CpMo(CO)_2(\mu\text{-}SR)\}_2$ dimers (Cp = η^5-C_5H_5; R = Me, t-Bu, Ph) was consistent with the interconversion of two different conformations of the molecules. The existence of geometrical *cis/trans* and *syn/anti* isomers of these complexes has long been known [7,8] but their electrochemical behaviour has not been previously investigated.

0022-328X/86/$03.50

Although there has been much interest in the electrochemical investigation of organometallic or coordination compounds which can exist in different isomeric forms [9], comparatively few reports have been devoted to dinuclear species [10–13]. Since our work is of relevance to problems relating to isomerisation accompanying electron-transfer, a subject reviewed recently [14], we present here the results of ^1H NMR and electrochemical studies of the title compounds, as well as the X-ray crystal structure of the dication, R = t-Bu. The methyl-thiolate bridged dimer was more extensively studied than the phenyl and t-butyl analogues. Nevertheless, the comparison of the electrochemical behaviour of the three complexes suggest that steric effects dictate the geometry of the neutral compounds.

Results and discussion

^1H NMR spectroscopy of the neutral dimers

The ^1H NMR spectrum of $\{CpMo(CO)_2(\mu\text{-}SMe)\}_2$ recorded at room temperature shows two sets of signals, each made up of two singlets, which are assigned to the resonances of the cyclopentadienyl and methyl protons (Table 1) of each isomer. *Syn / anti* isomerism for this kind of compound is generally not observable spectroscopically at room temperature [7], but the inversion at sulfur may be sufficiently slowed down to allow the *syn* and *anti* conformational isomers to be observed at low temperature. Variable temperature ^1H NMR spectroscopy of the methyl- and phenyl-thiolate bridged dimers leads to broadening, and eventually splitting of one of the cyclopentadienyl-protons resonances (−96 °C) [15]. Because of the presence of non-equivalent Cp ligands in the *trans* isomer, the signal which is affected by temperature is assigned to this species [16]. In agreement with the reported structure of the complex, R = Ph [7], the *trans*-$\{CpMo(CO)_2(\mu\text{-}SPh)\}_2$ isomer appears to be the major species in solution.

For the t-butyl thiolate analogue, variable temperature NMR does not afford conclusive evidence for the preferred geometry of the complex. Taking advantage of the fact that both neutral isomers are oxidized to a single dication (see electrochemistry below), we prepared the $\{CpMo(CO)_2(\mu\text{-}S\text{-}t\text{-}Bu)\}_2^{2+}$ complex and studied its crystal structure in order to determine its geometry.

The chemical oxidation of the $\{CpMo(CO)_2(\mu\text{-}SR)\}_2$ dimers and the X-ray crystal structure of $\{CpMo(CO)_2(\mu\text{-}S\text{-}t\text{-}Bu)\}_2^{2+}(BF_4^-)_2$

As shown by the redox potentials listed in Table 3, the neutral parents may be readily oxidized by mild oxidizing agents such as silver(I) ions or iodine. Treatment of the dimers with $AgBF_4$ (or $NOPF_6$) yields red crystalline materials (reaction 1) analysing for $\{Cp_2Mo_2(CO)_4(SR)_2\}(A^-)_2$ (A = PF_6 or BF_4), and behaving as 1 : 2 electrolytes.

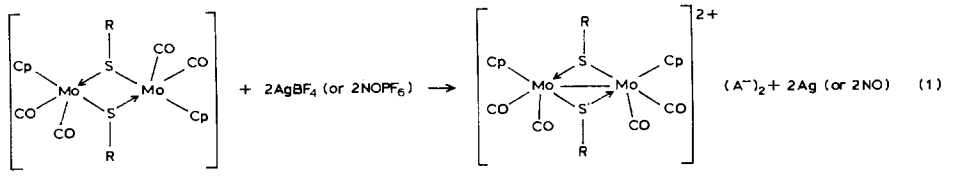

(R = Me , t-Bu , Ph)

TABLE 1

^1H NMR PARAMETERS FOR $\{CpMo(CO)_2(\mu\text{-}SR)\}_2$ AND ^1H AND ^{13}C NMR DATA FOR $[\{(CpMo(CO)_2(\mu\text{-}SR)\}_2]^{2+}(A^-)_2$ AT ROOM TEMPERATURE [a]

R	δ	%
Me	isomer *trans* 5.53 (s,10H); 1.94 (s,6H) isomer *cis* 5.37 (s,10H); 1.85 (s,6H)	57 [b] 43 [b]
Ph	isomer *trans* 5.35 (s,10H); 7.25 (m,10H) isomer *cis* 5.59 (s,10H); 7.45 (m,10H)	87 13
t-Bu	isomer *trans* 5.66 (s,10H); 1.37 (s,18H) isomer *cis* 5.55 (s,10H), 1.42 (s,18H)	80 20

$[\{(CpMo(CO)_2(\mu\text{-}SR)\}_2]^{2+}(A^-)_2$	$\delta(^1H)$	$\delta(^{13}C)$
M = Mo; R = Me; A = PF_6	6.26 (s,10H) 2.73 (s,6H)	215.8 (s,CO) 97.48 (s,C_5H_5) 29.34 (s,Me)
M = W; R = Me; A = PF_6	6.36 (s,10H) 2.92 (s,6H)	203.8 (s,CO) 94.52 (s,C_5H_5) 30.11 (s,Me)
M = Mo; R = Ph; A = BF_4	7.52 (m,10H) 6.48 (s,5H) 6.35 (s,5H)	
M = Mo; R = t-Bu; A = BF_4	6.42 (s,10H) 1.46 (m,9H)	

[a] The spectra were recorded with $CDCl_3$ solutions; frequencies are in ppm relative to external TMS. [b] See Ref. 16.

Pertinent ^1H and ^{13}C NMR data are listed in Table 1. These data and the shift of $\nu(CO)$ (see Experimental part) to higher frequencies relative to those of the 1:1 electrolytes are consistent with this formulation. To our knowledge, these relatively simple dicationic species are novel. However, the formation of $\{Cp_2Mo(\mu\text{-}SPh)_2MoCp_2\}^{2+}$ on electrochemical or chemical oxidation of $Cp_2Mo(SPh)_2$ in a non-coordinating solvent has been reported [17]. In $\{Cp_2Mo(\mu\text{-}SPh)_2MoCp_2\}^{2+}$ there is no metal–metal bond, whereas a single M–M bond is required to allow the metal centres to achieve an 18-electron configuration in the diamagnetic $\{CpMo(CO)_2(\mu\text{-}SR)\}_2^{2+}$ species.

In order to determine the geometry of the stable isomer at the (+2) level (see ^1H NMR and electrochemical studies) we have carried out an X-ray crystallographic structural analysis on $\{CpMo(CO)_2(\mu\text{-S-t-Bu})\}_2^{2+}(BF_4^-)_2 \cdot CH_3CN$.

The crystal structure of the complex consists of discrete dinuclear dications and BF_4 anions and CH_3CN (solvent) molecules. Selected bond distances and angles are listed in Table 2. The numbering scheme and a view of the dinuclear dicationic species are depicted in Fig. 1, from which it can be seen that the M_2S_2 core is

TABLE 2

BOND LENGTHS (Å) AND BOND ANGLES (°) (with e.s.d.'s)

Mo(1)---Mo(2)	3.008(2)		
S(1)---S(2)	2.789(6)		
Mo(1)–S(1)	2.458(4)	Mo(2)–S(1)	2.453(4)
Mo(2)–S(2)	2.456(4)	Mo(2)–S(2)	2.460(4)
Mo(1)–C(1)	2.008(13)	Mo(2)–C(3)	2.002(13)
Mo(1)–C(2)	2.026(16)	Mo(2)–C(4)	2.029(15)
C(1)–O(1)	1.135(13)	C(3)–O(3)	1.150(13)
C(2)–O(2)	1.129(14)	C(3)–O(4)	1.134(13)
Mo(1)–C(11)	2.337(15)	Mo(2)–C(21)	2.290(15)
Mo(1)–C(12)	2.282(15)	Mo(2)–C(22)	2.375(16)
Mo(1)–C(13)	2.283(17)	Mo(2)–C(23)	2.364(16)
Mo(1)–C(14)	2.309(16)	Mo(2)–C(24)	2.293(16)
Mo(1)–C(15)	2.359(16)	Mo(2)–C(25)	2.254(16)
C(11)–C(12)	1.412(15)	C(21)–C(22)	1.414(15)
C(12)–C(13)	1.416(15)	C(22)–C(23)	1.425(15)
C(13)–C(14)	1.449(16)	C(23)–C(24)	1.388(16)
C(14)–C(15)	1.440(15)	C(24)–C(25)	1.437(16)
C(15)–C(11)	1.410(15)	C(25)–C(21)	1.421(15)
S(1)–C(31)	1.886(13)	S(2)–C(41)	1.886(13)
C(31)–C(32)	1.560(16)	C(41)–C(42)	1.521(15)
C(31)–C(33)	1.479(15)	C(41)–C(43)	1.496(15)
C(31)–C(34)	1.518(16)	C(41)–C(44)	1.510(15)
B(1)–F(11)	1.374(15)	B(2)–F(21)	1.408(17)
B(1)–F(12)	1.366(15)	B(2)–F(22)	1.372(17)
B(1)–F(13)	1.377(16)	B(2)–F(23)	1.369(17)
B(1)–F(14)	1.398(16)	B(2)–F(24)	1.380(17)
C(5)–C(6)	1.452(15)	C(6)≡N	1.161(9)
Mo(1)–S(1)–Mo(2)	75.5(0.1)	Mo(1)–S(2)–Mo(2)	75.4(0.1)
Mo(1)–S(1)–C(31)	122.3(0.6)	Mo(1)–S(2)–C(41)	123.4(0.5)
Mo(2)–S(1)–C(31)	124.0(0.5)	Mo(2)–S(2)–C(41)	123.7(0.5)
S(1)–Mo(1)–S(2)	69.2(0.1)	S(1)–Mo(2)–S(2)	69.2(0.1)
C(1)–Mo(1)–C(2)	80.2(0.8)	C(3)–Mo(2)–C(4)	81.5(0.8)
C(1)–Mo(1)–S(1)	90.8(0.6)	C(3)–Mo(2)–S(1)	91.0(0.5)
C(1)–Mo(1)–S(2)	137.9(0.5)	C(3)–Mo(2)–S(2)	141.8(0.5)
C(2)–Mo(1)–S(1)	141.1(0.6)	C(4)–Mo(2)–S(1)	139.5(0.6)
C(2)–Mo(1)–S(2)	92.5(0.6)	C(4)–Mo(2)–S(2)	92.6(0.5)
Mo(1)–C(1)–O(1)	173.8(1.7)	Mo(2)–C(3)–O(3)	172.5(1.5)
Mo(1)–C(2)–O(2)	171.1(1.9)	Mo(2)–C(4)–O(4)	176.3(1.8)
G(1)–Mo(1)–Mo(2) [a]	161.1(2)		
G(2)–Mo(2)–Mo(1) [a]	160.9(2)		

Least-squares mean planes:

1 Ring (C(11)–C(14)) (planarity within 0.001 Å)

2 Ring (C(21)–C(25)) (planarity within 0.015 Å)

3 Mo(1)–Mo(2)–S(1)

4 Mo(1)–Mo(2)–S(2)

5 Internal bisecting plane of 3–4

6 O(1)–Mo(1)–Mo(2)–O(3) (planarity within 0.03 Å)

7 O(2)–Mo(1)–Mo(2)–S(2) (planarity within 0.03 Å)

TABLE 2 (continued)

Dihedral angles					
1–2	31.9(1)	1–3	78.3(1)	1–4	78.0(1)
2–3	78.0(1)	2–4	80.2(1)	3–4	88.2(1)
1–5	90.3(1)	2–5	91.5(1)	3–7	7.5(1)
4–6	6.1(1)	6–7	102.0(1)		
Angles between bonds and mean planes					
Mo(1)–Mo(2)–1		73.4			
Mo(1)–Mo(2)–2		74.7			
Torsion angles					
O(1)–Mo(1)–Mo(2)–O(3)			177.0(1.0)		
O(1)–Mo(1)–Mo(2)–O(4)			173.0(1.0)		

[a] G(1) and G(2) are respectively the centroids of the cyclopentadienyl rings 1 and 2.

sandwiched between the two cyclopentadienyl rings. The butterfly $Mo_2(\mu\text{-}S)_2$ unit is of a well established structural type [18]. The atoms S(1) and S(2) subtend the same *cis* angles of 69.2(1)° at Mo(1) and Mo(2). The thiolate bridges are very nearly symmetric. The carbonyl groups are in a *cis* configuration with respect to the Mo–Mo line and are on the opposite side of the t-BuS units relative to that edge. The Mo–Mo bond length is within the range regarded as typical of single bonds [19]. However, the Mo–Mo distance is significantly longer than in another Mo^{III}–Mo^{III} complex, $\{CpMo(CO)(\mu\text{-}SMe)_3Mo(CO)Cp\}Br$ (2.785 Å) [19], but this is a characteristic feature associated with a decrease in the number of bridging sulfur atoms. The Mo–S–Mo angles (ca. 75.4°) subtended at the μ-S atoms are comparable to those required for a structure in which a metal–metal interaction exists [20].

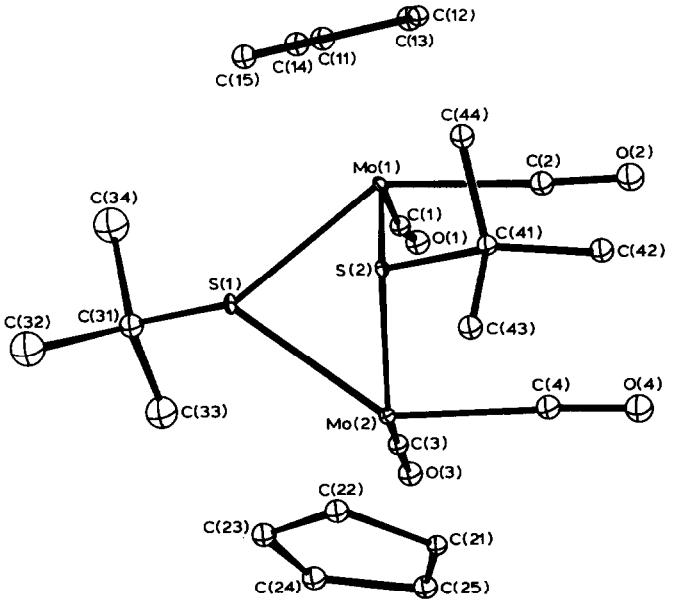

Fig. 1. ORTEP view of the bimetallic dicationic species. Thermal ellipsoids and spheres enclose 25% probability.

A strong S–S intramolecular interaction (2.789(6) Å) is observed, the S–S bond length being shorter than those in the triply bridging compounds {CpMo(CO)(μ-SMe)$_3$Mo(CO)Cp}Br (2.80(1) and 3.00(1) Å [19]) and [(η^7-C_7H_7)Mo(μ-S-t-Bu)$_3$Mo(CO)$_2${P(OMe)$_3$}] (3.256(3) and 2.939(3) Å, [20a]).

The coordination at each Mo atom may be described as distorted pyramidal; the two pyramids share a common edge defined by two t-BuS ligands. The metallic atom is capped by a cyclopentadienyl unit. The C_5H_5 rings are planar and form a dihedral angle of 31.9(1)°. The Mo–Mo axis is shifted of 19(1)° from the normal direction of each plane. To our knowledge this is the first dicationic Mo^{III} dimer doubly bridged by alkyl sulfides groups to have been structurally characterized by an X-ray analysis.

Oxidative electrochemistry of the {CpMo(CO)$_2$(μ-SR)}$_2$ dimers

The trans^{2+} → cis^{2+} isomerization

Figures 2a and 2b present the cyclic voltammograms of the oxidation of the dimers (R = Me and Ph respectively) in thf/{Bu_4N}{PF_6} (0.2 *M*). The t-butyl thiolate bridged dimer shows a behaviour qualitatively similar to that of the phenyl analogue. The data listed in Table 3 demonstrate that there is no important solvent effect on the oxidation potentials of the dimers.

From Fig. 2 it can be seen that the isomers, the distribution of which is strongly affected by the nature of the R group [16], are oxidized at distinct potentials. On the basis of ^{1}H NMR data (R = Me, Ph) and in accord with the structure and cyclic

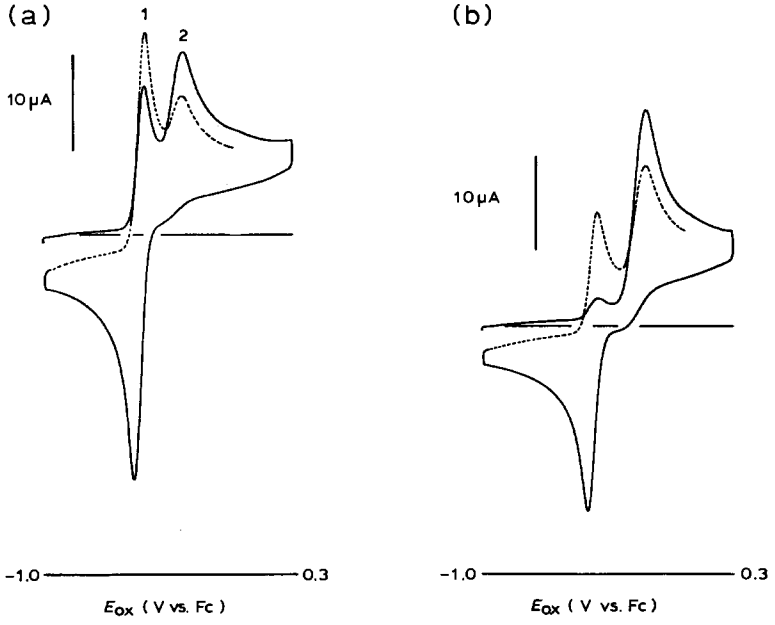

Fig. 2. Cyclic voltammograms for ca. 0.5 m*M* solutions of (a) {CpMo(CO)$_2$(μ-SMe)}$_2$ and (b) {CpMo(CO)$_2$(μ-SPh)}$_2$ dimers in thf/{Bu_4N}{PF_6} (0.2 *M*) (v 0.2 V s^{-1}, vitreous carbon disc electrode).

TABLE 3

ELECTROCHEMICAL DATA FOR THE OXIDATION OF $\{CpM(CO)_2(\mu\text{-SR})\}_2$ COMPLEXES [a]

M	R	Solvent	*cis*-Isomer		*trans*-Isomer	
			$E_{ox}^{1/2}$ (V vs. Fc)	ΔE_p (mV)	E_{ox} (V vs. Fc)	$E_{p/2}$ (V vs. Fc)
Mo	Me	thf	−0.54	40	−0.32	−0.37
		CH_3CN	−0.52	35	−0.36	−0.41
		CH_2Cl_2	−0.49	40	−0.32	−0.37
		PC	−0.55	40	−0.36	−0.42
W	Me	thf	−0.71	60	−0.41	−0.50
		CH_3CN	−0.67	35	−0.41	−0.49
		CH_2Cl_2	−0.63	35	−0.41	−0.46
Mo	t-Bu	thf	−0.54	40	−0.19	−0.24
		CH_3CN	−0.50	35	−0.23	−0.28
		CH_2Cl_2	−0.47	60	−0.20	−0.24
		PC	−0.50	35	−0.16	−0.21
Mo	Ph	thf	−0.44	40	−0.13	−0.20
		CH_3CN	−0.41	35	−0.19	−0.24
		CH_2Cl_2	−0.37	35	−0.17	−0.22

[a] Potentials quoted against the Fc/Fc^+ couple.

voltammetry (CV) of the dication (R = t-Bu), the first oxidation process was assigned to the *cis* complex. While the oxidation of the *cis* isomer appears highly reversible from cyclic voltammetry, the oxidation of *trans*-$\{CpMo(CO)_2(\mu\text{-SR})\}_2$ is

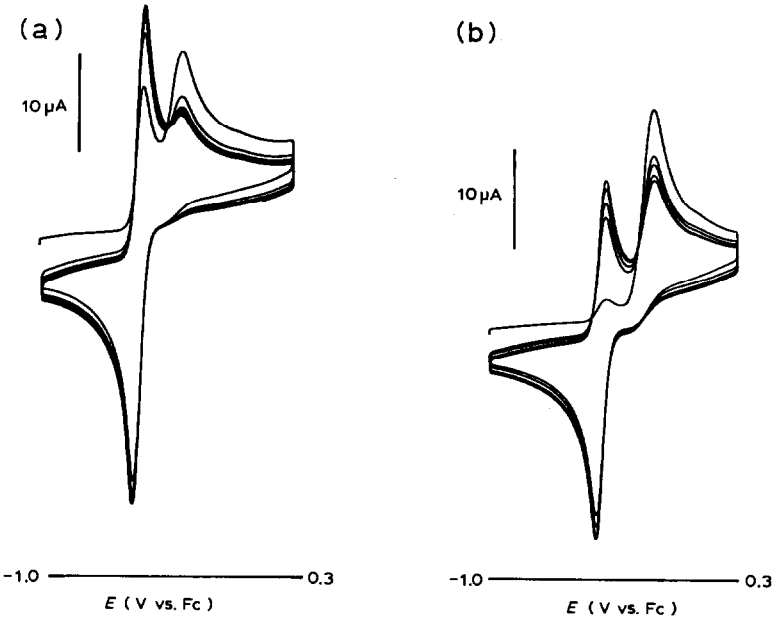

Fig. 3. Multiple scans cyclic voltammetry for ca. 0.5 m*M* solutions of (a) $\{CpMo(CO)_2(\mu\text{-SMe})\}_2$ and (b) $\{CpMo(CO)_2(\mu\text{-SPh})\}_2$ dimers in thf/0.2 $M\{Bu_4N\}\{PF_6\}$ (v 0.2 V s^{-1}).

not, even at low temperature or moderately fast scan rate, v, 1 V $s^{-1} < v < 2$ V s^{-1}. This suggests the occurrence of a fast chemical step subsequent to the electron transfer event. Multiple scans cyclic voltammetry of the dimers (R = Me and Ph in Fig. 3) demonstrates that the only reaction observed on the time-scale of the experiment is the conversion of the harder to oxidize (i.e. *trans*) isomer into the other one, the sum of the concentrations of the isomers remaining constant. The presence of isopotential points on the CV traces indicates that no side reaction is taking place and that the same number of electrons are involved in both oxidation processes [13]. These observations demonstrate that the chemical step responsible for the observed behaviour is a fast geometrical isomerisation, e.g. eq. 2.

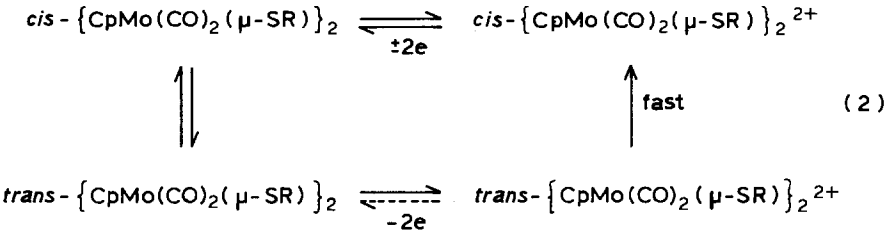

The number of electrons involved in the oxidation processes was derived from cyclic voltammetry and potential step experiments conducted on the oxidized *cis* species, R = Me. The calculated n value [21] is close to 2 ($n = 1.9$ at 0.02 V s^{-1}, $n = 1.65$ at 0.2 V s^{-1}) in accord with the anodic to cathodic peak separation for the reversible couple (Table 3; $\Delta E_p = E_{p,a} - E_{p,c}$ for ferrocene is 60–80 mV in CH_2Cl_2 and thf and ca. 60 mV in CH_3CN and PC).

As expected from cyclic voltammetry, controlled-potential electrolyses (CPE) of the title compounds at the potential of the second oxidation step convert the mixture of the neutral isomers into a single species, e.g. *cis*-$\{CpMo(CO)_2(\mu\text{-}SR)\}_2^{2+}$. Coulometric experiments reveal that the cell current decays linearly with the charge passed. The number of electrons transferred in the process is less than two, and is slightly dependent on the concentration of the starting material (R = Me) (Table 4). The values of n_{app} and the estimated yield [23] of *cis*-$\{CpMo(CO)_2(\mu\text{-}SMe)_2\}^{2+}$ are consistent with the stoichiometry of the overall reaction 3 (Table 4).

$$(cis + trans)\text{-}\{CpMo(CO)_2(\mu\text{-}SMe)\}_2 - (1 + x)e \rightarrow x\ cis\text{-}\{CpMo(CO)_2(\mu\text{-}SMe)\}_2^{2+} + \text{products} \quad (3)$$

In addition to the reversible system of the $cis^{0/2+}$ couple, the cyclic voltammogram of the anolyte shows the presence of a small peak ($E_p \sim -2.3$ V) which we assign to the reduction of a by-product of the oxidation of $\{CpMo(CO)_2(\mu\text{-}SMe)\}_2$. This additional peak is suppressed on reduction back to the neutral dimer (potential of electrolysis: -1.0 V).

Oxidations by loss of two electrons at the same potential have been reported for other dinuclear complexes possessing the M_2S_2 (M = Mo, W [4,5]) or Fe_2P_2 [24] cores. This was assigned to the formation of a single metal–metal bond and structural rearrangement [4,5,24], which is entirely consistent with our observations

TABLE 4

COULOMETRIC DATA FOR THE OXIDATION OF $\{CpMo(CO)_2(\mu\text{-}SR)\}_2$ DIMERS IN thf/$\{Bu_4N\}\{PF_6\}$ (0.2 *M*)

R	Concentration of complex (m*M*)	n_{app} ($F\ mol^{-1}$)	Yield of dication (%) [a]
Me	0.30	1.6_4	64
	0.43	1.5_4	65
	0.52	1.6_3	69
	0.62	1.7_0	69
	0.65	1.7_0	72
	0.72	1.7_2	71
	1.04	1.8_3	82
t-Bu	0.36	1.9_0	–
Ph	0.31	1.5_6	–
	0.41	1.6_6	–

[a] Calculated from cyclic voltammetry [23].

(geometrical isomerization, decrease of the Mo–Mo separation from 3.940(2) Å in $\{CpMo(CO)_2(\mu\text{-}SPh)\}_2$ [7] to 3.008(2) Å in $\{CpMo(CO)_2(\mu\text{-S-t-Bu})\}_2^{2+}$, Table 2). It can be seen from Table 3 that both the metal and the sulfur substituent (R = Me, Ph) have marked effects on the redox potentials of both *cis* and *trans* isomers, the phenyl-thiolate bridged dimer being, as expected, harder to oxidise than the methyl analogue. The substantial substituent effect suggests that in these dimers, as in $\{CpMo(NO)(\mu\text{-}SR)\}_2$ [25], the HOMO possesses metal and sulfur character. We believe this is consistent with the isomerisation occurring through cleavage of a Mo–S–Mo bridge [26].

The cis ⇆ trans interconversion of the neutral isomers

The isomerization of the neutral compounds is detected by electrochemical means although the reactions are much slower than at the (+2) level.

The *trans* → *cis* conversion for the methyl-thiolate dimer is evidenced by controlled-potential oxidation of the mixture of the neutral isomers at the potential of the first wave, as well as by ramp-clamp-reverse ramp [27] cyclic voltammetry (Fig. 4). The decay of the concentration of *trans*-$\{CpMo(CO)_2(\mu\text{-}SMe)\}_2$ on oxidizing at E_{ox_1} (a potential at which this species is not electroactive, Scheme 1) and the increase in the oxidation peak current of *cis*-$\{CpMo(CO)_2(\mu\text{-}SMe)\}_2$ on the second scan (Fig. 4) must result from a *trans* → *cis* shift of the equilibrium between the neutral isomers and/or from the occurrence of the cross-redox reaction (eq. 4).

$$\begin{array}{l} cis\text{-}\{CpMo(CO)_2(\mu\text{-}SMe)\}_2^{2+} + trans\text{-}\{CpMo(CO)_2(\mu\text{-}SMe)\}_2 \\ \qquad\qquad\qquad\qquad\qquad\qquad \uparrow\!\downarrow K_{eq} \\ cis\text{-}\{CpMo(CO)_2(\mu\text{-}SMe)\}_2 + trans\text{-}\{CpMo(CO)_2(\mu\text{-}SMe)\}_2^{2+} \end{array} \qquad (4)$$

Although the magnitude of K_{eq} [28] illustrates that the forward reaction is thermodynamically disfavoured, the fast $trans^{2+} \rightarrow cis^{2+}$ isomerisation could effectively drive it in this direction.

That the reverse reaction (i.e. *cis* → *trans*) also takes place is shown by controlled-potential electrolyses of the *cis* dication (R = Me, Ph, t-Bu) which regener-

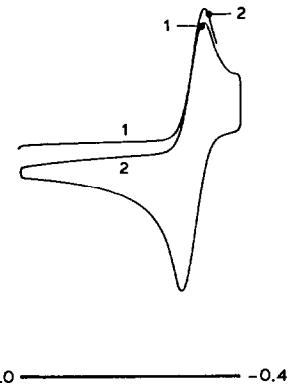

Fig. 4. Ramp-clamp cyclic voltammetry of $\{CpMo(CO)_2(\mu\text{-}SMe)\}_2$ in PC $\{Bu_4N\}\{PF_6\}$ (0.1 *M*). (1: first cycle; 2: second scan after 10 s hold at −0.4 V).

ates a mixture of the neutral isomers. The *cis* → *trans* conversion is a slow process, which is not detected by slow scan cyclic voltammetry of the dication (v 0.02 V s^{-1}) and whose rate is strongly affected by the nature of the R substituent, as shown by the following observations:

(i) Although it is not thermodynamically favoured, the *cis* isomer is largely represented in the samples of the dimer, R = Me [16], whereas it is a minor species for R = Ph and t-Bu. As shown by the data in Table 3, the substitution of t-Bu for Me has no important effect on the oxidation potential of the *cis* isomer. On the contrary, $\Delta E_{p/2}$ indicates that the neutral *trans* isomer is favoured to a much greater extent with t-BuS than with MeS as a ligand [29].

(ii) On oxidation of $\{CpMo(CO)_2(\mu\text{-}SR)\}_2$ (*cis* + *trans*) to the *cis* dication and reverse reduction to the neutral species, the initial *cis*/*trans* ratio is restored (or nearly so) for R = Ph and t-Bu whereas it increases for R = Me.

(iii) Whereas the diffusion layer is depleted of almost all of the *trans* isomer (R = Me) on repetitive CV, both *cis* and *trans* remain present at the electrode under steady state conditions for R = Ph and t-Bu (Fig. 3). Owing to the irreversibility of the oxidation of the *trans* isomer in all three cases, this observation indicates that the neutral isomers equilibrate more rapidly for R = Ph and t-Bu than for R = Me.

The above observations (i–iii) suggest that the kinetic stability of *cis*-$\{CpMo(CO)_2(\mu\text{-}SMe)\}_2$ compared with that of its phenyl- and t-butyl counterparts is steric rather than electronic in origin. For mononuclear carbonyl [9h,30,31] or

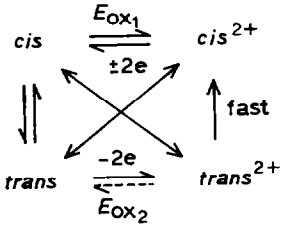

SCHEME 1

dinitrogen [9h,30] $Mo(L)_2(dppe)_2$ complexes, the *cis* or *trans* arrangement of the L ligands (CO or N_2) depends on the balance between steric and electronic factors [1c,9b]. This appears to be the case for the $\{CpMo(CO)_2(\mu\text{-}SR)\}_2$ dimers as well, and it may be inferred from the discussion above that steric crowding is responsible for the preferred *trans* geometry of the neutral dimers, whilst electronic factors favour the *cis* conformation at the (+2) level.

The overall isomerization process as we envisage it is summarized in Scheme 1 (the crossed arrows represent the cross-redox reaction, eq. 4). The process is clearly not catalytic since the stable cis^{2+} (and not cis^0) isomer is produced on oxidation of the neutral *trans* dimer. It is the first reported example of a geometrical isomerisation of dinuclear SR-bridged compounds induced by the transfer of two electrons at the same potential.

Experimental

All the experiments (preparations, electrochemistry) were carried out under N_2 or Ar.

Syntheses

The neutral $\{CpMo(CO)_2(\mu\text{-}SR)\}_2$ dimers were prepared by published procedures [32]. Standard Schlenk techniques were used for preparative experiments. Florisil was used for chromatographic separation and purifications.

Preparation of the dicationic complexes $[\{CpM(CO)_2(\mu\text{-}SR)\}_2](A)_2$ (M = Mo or W, R = Me, A = PF_6; M = Mo, R = Ph or Bu^t, A = BF_4)

Method 1 (A = PF_6). A solution of 1 g (1.9×10^{-3} mol, M = Mo or 1.4×10^{-3} mol, M = W) of $\{CpM(CO)_2(\mu\text{-}SMe)\}_2$ in 50 ml of thf was made up under nitrogen then added to a solution of 1 g (5.7×10^{-3} mol) of $NOPF_6$ in 30 ml of thf. 3 h stirring at room temperature gave a red precipitate of $[\{CpMo(CO)_2(\mu\text{-S-t-Bu})\}_2](PF_6)_2$ which was filtered off, washed twice with thf, and dried (yield ca. 65%). The brown filtrate yielded only intractable products.

Anal. found for molybdenum complex: C, 23.7; F, 24.5; Mo, 23.0; S, 7.2. $C_{16}H_{16}F_{12}Mo_2O_4P_2S_2$ calcd.: C, 23.5; F, 27.8; Mo, 23.4; S, 7.8%. IR (CH_2Cl_2): ν(CO) 2110s, 2070s. Molar conductivity: (in nitromethane, $c\,10^{-3}$ *M*): 165 Ω mol^{-1} cm^{-1}.

Anal. found for tungsten complex: C, 19.8; F, 22.1; S, 5.8, W, 35.8. $C_{16}H_{16}F_{12}O_4P_2S_2W_2$ calcd.: C, 19.4; F, 22.9; S, 6.4; W, 37.0%. IR (CH_2Cl_2), ν(CO): 2095s, 2050s. Molar conductivity (in nitromethane, $c\,10^{-3}$ *M*): 179 Ω mol^{-1} cm^{-1}.

Method 2 (A = BF_4). A solution of silver tetrafluoroborate (2×10^{-3} mol) in 5 ml of thf was added to a solution of $\{CpMo(CO)_2(\mu\text{-}SR)\}_2$ (R = Ph, t-Bu) (10^{-3} mol) in 30 ml of CH_2Cl_2. The mixture was stirred for a few minutes. The solvents were then evaporated and CH_3CN was added to the residue. Metallic silver was filtered off and CH_2Cl_2 was added to the filtrate. After a few hours at low temperature, red-brown crystals of $[\{CpMo(CO)_2(\mu\text{-}SR)\}_2](BF_4)_2 \cdot CH_3CN$ precipitated.

Complex, R = Ph: IR (CH_2Cl_2), ν(CO): 2090s, 2040s.

Complex, R = t-Bu: IR (CH_2Cl_2), ν(CO): 2095s, 2055s.

Electrochemistry

The solvents used for the syntheses and electrochemical studies (tetrahydrofuran: thf; methylene chloride: CH_2Cl_2; propylene carbonate: PC) were purified by standard procedures [33]. Methyl cyanide (CH_3CN, Carlo Erba reagent for HPLC) was used without further purification.

Tetrabutylammonium hexafluorophosphate was used as supporting electrolyte. The solutions were 0.2 *M* in $\{Bu_4N\}\{PF_6\}$ for thf or CH_2Cl as solvent but 0.1 *M* for CH_3CN or PC. The purification of the salt has been previously described [33].

The electrochemical apparatus as well as the experimental techniques were as described previously [33]. All the potentials in text, tables and figures are quoted relative to ferrocene which was added as an internal standard at the end of the experiments.

NMR and infrared spectroscopies

^1H and ^{13}C NMR spectra were recorded with a JEOL FX 100 with a Fourier transform spectrometer. TMS was used as a reference.

The infrared spectra, either in solution or as Nujol mull were recorded with a Pye Unicam SP 2000 spectrometer.

Crystal structure analysis of $\{Cp(CO)_2\overline{Mo(\mu\text{-}S\text{-}t\text{-}Bu)_2}Mo(CO)_2Cp\}(BF_4)_2 \cdot CH_3CN$

$C_{24}H_{31}B_2F_8Mo_2NO_4S_2$, $M = 827.1$. Orthorhombic, space group $P2_12_12_1$, a 10.598(3), b 13.489(3), c 21.801(3) Å, V 3116(6) Å^3, $Z = 4$, D_c 1.76 g cm^{-3}, Mo-K_α radiation, λ 0.71069 Å, μ(Mo-K_α) 1 mm^{-1}.

A small crystal of $\{Cp(CO)_2\overline{Mo(\mu\text{-}S\text{-}t\text{-}Bu)_2}Mo(CO)_2Cp\}(BF_4) \cdot CH_3CN$, of dimensions ca. $0.2 \times 0.2 \times 0.1$ mm sealed in a capillary tube, was examined on a Enraf–Nonius CAD4 automatic four-circle diffractometer (Centre de Diffusion Automatique de Lyon I), with graphite monochromated Mo-K_α radiation. All measurements were made at room temperature. Unit cell dimensions were refined by least-squares methods from setting angles of 25 reflections ($15 < \theta < 25°$). The intensities of 4423 independent reflections ($0 \leqslant h \leqslant 14$; $0 \leqslant k \leqslant 18$; $0 \leqslant l \leqslant 21$) with $2\theta < 60°$ were collected using the ω–2θ scan method. One standard reflection (2 $\bar{2}$ 3), scanned every 100 reflections, was used to place the intensity data on a common scale and no systematic variations in this standard were observed. Lp corrections were applied but no absorption correction. 2401 reflections, with $F > 4\sigma(F)$, were considered as observed and used in the structure refinement. The systematic absences ($h00 \rightarrow h = 2n + 1$; $0k0 \rightarrow k = 2n + 1$; $00l \rightarrow l = 2n + 1$) observed on Buerger and Weissenberg photographs were confirmed on the diffractometer data. Therefore, the space group must be the non-symmetric $P2_12_12_1$ group. A sharpened Patterson map was produced (in SHELX) [34], and revealed clearly the position of the Mo–Mo bond (~ 3.00 Å). The analysis of the main interatomic peaks provided a solution for the location of the two independent Mo atoms. After refinements of their atomic coordinates the R was 0.25. Subsequent refinements using full-matrix least-squares and difference Fourier syntheses enabled us to determine the positions of all non-hydrogen atoms. In the final refinements with anisotropic Mo and S atoms and isotropic all other non-hydrogen atoms (193 parameters), the R and R_w values were respectively 0.060 and 0.059 (weighting scheme $w = 2.05 / \{\Sigma\sigma^2(F_0) +$

$0.0001F_0^2\}|$. Some hydrogen atoms were evident in the final difference Fourier map ($+1.2 < \rho < -0.6$ e Å^{-3}) but no attempt was made to locate them.

The final atomic coordinates and the isotropic thermal parameters are given in Table 5.

TABLE 5

FRACTIONAL ATOMIC COORDINATES ($\times 10^4$) (with e.s.d.'s) AND EQUIVALENT ISOTROPIC THERMAL PARAMETERS (Å$^2 \times 10^4$) (with e.s.d.'s) [a]

Atom	x	y	z	U_{eq}
Mo(1)	1516(1)	351(1)	−612(1)	324(7)
Mo(2)	1350(1)	−1103(1)	−1655(1)	310(7)
S(1)	−375(3)	−485(3)	−1010(2)	337(23)
S(2)	1761(4)	−1459(3)	−567(2)	325(22)
C(1)	1367(19)	1407(11)	−1257(6)	454(45)
O(1)	1361(15)	2051(9)	−1591(6)	674(38)
C(2)	3365(15)	560(15)	−808(8)	616(55)
O(2)	4363(13)	804(11)	−912(6)	822(49)
C(3)	1122(17)	25(11)	−2241(6)	490(50)
O(3)	1042(12)	605(9)	−2626(5)	600(38)
C(4)	3195(13)	−815(13)	−1828(9)	549(55)
O(4)	4222(13)	−687(10)	−1951(6)	668(41)
C(31)	−1779(13)	223(12)	−1312(6)	518(51)
C(32)	−2868(30)	−504(22)	−1141(13)	1615(143)
C(33)	−1701(27)	433(20)	−1977(8)	1215(98)
C(34)	−1989(33)	1158(19)	−938(13)	1587(144)
C(41)	3235(13)	−2091(11)	−280(6)	473(48)
C(42)	4460(16)	−1682(13)	−542(8)	624(55)
C(43)	3088(18)	−3156(12)	−455(8)	590(55)
C(44)	3191(17)	−1934(13)	405(6)	536(53)
C(11)	1213(16)	189(13)	445(6)	537(52)
C(12)	2301(16)	763(12)	329(6)	491(52)
C(13)	1960(18)	1649(13)	23(9)	656(63)
C(14)	601(17)	1610(12)	−49(8)	542(54)
C(15)	151(16)	698(13)	215(8)	572(57)
C(21)	1984(16)	−2591(11)	−2055(6)	465(49)
C(22)	953(16)	−2835(12)	−1671(9)	593(57)
C(23)	−106(16)	−2348(13)	−1940(8)	568(57)
C(24)	243(16)	−1798(13)	−2451(6)	576(55)
C(25)	1572(18)	−1959(13)	−2536(6)	661(59)
B(1)	5916(18)	669(13)	835(8)	824(88)
F(11)	7018(13)	1045(11)	598(6)	1195(53)
F(12)	5510(15)	−160(11)	535(6)	1290(55)
F(13)	6069(13)	462(11)	1449(6)	1186(52)
F(14)	4982(13)	1401(11)	838(6)	1381(64)
B(2)	3974(23)	1511(17)	−2974(10)	1341(149)
F(21)	3688(17)	1374(11)	−2349(6)	1315(55)
F(22)	3696(20)	631(13)	−3259(8)	1941(85)
F(23)	3203(19)	2252(13)	−3182(9)	1743(85)
F(24)	5235(19)	1750(19)	−3027(10)	2548(132)
C(5)	−1125(22)	1212(20)	1855(11)	1062(90)
C(6)	98(21)	1640(17)	1714(11)	819(74)
N	983(20)	2038(17)	1522(10)	390(27)

[a] For Mo and S atoms the thermal factor was of the form $T = \exp\{-2\pi^2(U_{11}h^2a^{*2} + \cdots 2\ U_{12}hka^*b^*)$ and $U_{eq} = (U_{11}U_{22}U_{33})^{1/3}$. For other atoms, $U_{eq} = U_{iso}$.

Acknowledgements

The CNRS (Centre National de la Recherche Scientifique) is acknowledged for financial support. The authors are grateful to Mr J.Y. Le Gall for assistance in NMR experiments.

References

1 For leading references see (a) R.H. Holm, Chem. Soc. Rev., 10 (1981) 455 and references therein; (b) S.J.N. Burgmayer and E.I. Stiefel, J. Chem. Educ., 62 (1985) 943 and references cited therein; (c) E.I. Stiefel, Prog. Inorg. Chem., 22 (1977) 1 and references therein.
2 (a) J.R. Dilworth in A. Muller and B. Krebs (Eds.), Sulfur, its Significance for Chemistry, for the Geo-, Bio- and Cosmosphere and Technology, Studies in Inorg. Chem., 5 (1984) 141 and references therein; (b) A.G. Wedd, ibid., 5 (1984) 181 and references therein.
3 F.A. Schultz, D.A. Ledwith and L.O. Leazenbee in D.T. Sawyer (Ed.), Electrochemical Studies of Biological Systems, Washington D.C., 1977, chapter 6, pp. 78–96 and references therein.
4 B. Zhuang, J.W. McDonald, F.A. Schultz and W.E. Newton, Organometallics, 3 (1984) 943.
5 B. Zhuang, J.W. McDonald, F.A. Schultz and W.E. Newton, Inorg. Chim. Acta, 99 (1985) L29.
6 O.A. Rajan, M. McKenna, J. Noordik, R.C. Haltiwanger and M. Rakowski DuBois, Organometallics, 3 (1984) 831.
7 I.B. Benson, S.D. Killops, S.A.R. Knox and A.J. Welch, J. Chem. Soc., Chem. Commun., (1980) 1137 and references therein.
8 P. Jaitner and H. Wohlgenannt, Inorg. Chim. Acta, 101 (1985) L43.
9 For leading references see (a) A.M. Bond, D.J. Darensbourg, E. Mocellin and B.J. Stewart, J. Am. Chem. Soc., 103 (1981) 6227 and references therein; (b) A.M. Bond, S.W. Carr and R. Colton, Organometallics, 3 (1984) 541; Inorg. Chem., 23 (1984) 2343; (c) R.D. Rieke, H. Kojima and K. Ofele, J. Am. Chem. Soc., 98 (1976) 6735. Angew. Chem., Int. Ed. Engl., 19 (1980) 538; (d) K.A. Connor and R.A. Walton, Organometallics, 2 (1983) 169; (e) J. Moraczewski and W.E. Geiger, J. Am. Chem. Soc., 103 (1981) 4779; (f) B.P. Sullivan and T.J. Meyer, Inorg. Chem., 21 (1982) 1037; (g) R.A. Rader and D.R. McMillin, Inorg. Chem., 18 (1979) 545. (h) J. Chatt, C.T. Kan, G.J. Leigh, C.J. Pickett and D.R. Stanley, J. Chem. Soc., Dalton Trans., (1980) 2032.
10 A.R. Hendrickson, J.M. Hope and R.L. Martin, J. Chem. Soc., Dalton Trans., (1976) 2032.
11 N.G. Connelly, G.A. Johnson, B.A. Kelly and P. Woodward, J. Chem. Soc., Chem. Commun., (1977) 436.
12 G. Bunzey, J.H. Enemark, J.K. Howie and D.T. Sawyer, J. Am. Chem. Soc., 99 (1977) 4168.
13 J.G. Gaudiello, T.C. Wright, R.A. Jones and A.J. Bard, J. Am. Chem. Soc., 107 (1985) 888 and references therein.
14 W.E. Geiger, Prog. Inorg. Chem., 33 (1985) 275.
15 One of the methyl singlets is also split at low temperature.
16 For the $\{CpMo(CO)_2(\mu\text{-SMe})\}_2$ dimer, the *cis/trans* ratio varies from one sample to another. One of our preparations yielded an almost pure isomer which appeared to be the *cis* one as judged from its variable temperature ^1H NMR spectrum (which was unaffected by lowering the temperature). The *cis/trans* ratio (R = Me) is also dependent on the solvent, the *trans* isomer being by 6–8% more abundant in CH_3CN than in thf.
17 J.C. Kotz, W. Vining, W. Coco, R. Rosen, A.R. Dias and M.H. Garcia, Organometallics, 2 (1983) 68.
18 See for examples: (a) W.A. Herrmann, H. Biersack, M.L. Ziegler and B. Balbach, J. Organomet. Chem., 206 (1981) C33; (b) G. Le Borgne and R. Mathieu, J. Organomet. Chem., 208 (1981) 201.
19 M.B. Gomes de Lima, J.E. Guerchais, R. Mercier and F.Y. Pétillon, Organometallics, submitted.
20 (a) I.B. Benson, S.A.R. Knox, P.J. Naish and A.J. Welch, J. Chem. Soc., Dalton Trans., (1981) 2235; (b) C. Couldwell, B. Meunier and K. Prout, Acta Cryst., B35 (1979) 603; (c) J.L. Le Quéré, F.Y. Pétillon, J.E. Guerchais, Lj. Manojlović-Muir, K.W. Muir and D.W.A. Sharp, J. Organomet. Chem., 249 (1983) 127; (d) A. Bino, F.A. Cotton, Z. Dori and J.C. Sekutowski, Inorg. Chem., 17 (1978) 2946.
21 n values were calculated according to Ref. 22: $n = (i_p F)^2/(2.69\ 10^5\ p^2\pi \cdot v)$ i_p and v are the peak current and scan rate in cyclic voltammetry. p is the slope of the chronoamperometric line $i(t) = f(t^{-1/2})$ $p = n\ F\ A\ D_0^{1/2}\ C_0\ \pi^{1/2}$.
22 A.J. Bard and L.R. Faulkner (Eds.) in Electrochemical Methods - Fundamental and Applications, John Wiley, New York, 1980.

23 The amount of dication formed on electrochemical oxidation was derived from comparison of the reduction peak currents of the reversible system ($cis^{2+} \rightarrow cis^{0}$) after electrolysis and before electrolysis, under steady-state conditions.
24 J.P. Collman, R.K. Rothrock, R.G. Finke, E.J. Moore and F. Rose-Munch, Inorg. Chem., 21 (1982) 146.
25 P.D. Frisch, M.K. Lloyd, J.A. McCleverty and D. Seddon, J. Chem. Soc., Dalton Trans., (1973) 2268.
26 Not inconsistent with this, controlled-potential oxidations of $\{CpMo(CO)_2(\mu\text{-}SR)\}_2$ (R = Me, Ph) in CH_3CN lead to the formation of a by-product containing bound CH_3CN molecule(s). This suggests the opening of a coordination site at some stage of the isomerisation process. M. Guéguen, F.Y. Pétillon and J. Talarmin, unpublished results.
27 (a) T.I. Al Salih, C.J. Pickett, R.L. Richards, J. Talarmin and A.J.L. Pombeiro, Portugaliae Electrochim. Acta, 3 (1985) 35; (b) T.I. Al Salih and C.J. Pickett, J. Chem. Soc., Dalton Trans., (1985) 1255.
28 $K_{eq} = |cis||trans|^{2+}/|cis^{2+}||trans| < 5\times10^{-7}$. That it is possible only to give an upper limit for K_{eq} is a result of the fact that the observed potential for the $trans^{0/2+}$ couple is shifted with respect to its thermodynamic value because of the subsequent $trans^{2+} \rightarrow cis^{2+}$ isomerisation.
29 It must be kept in mind that $E_{p/2}$ values are not thermodynamic potentials. The difference between the oxidation potentials of the *trans* isomer (R = Me, t-Bu) may be partly due to a faster $trans^{2+} \rightarrow cis^{2+}$ reaction for R = Me than for R = t-Bu.
30 T.A. George and C. Seibold, Inorg. Chem., 12 (1973) 2548.
31 A.M. Bond, B.S. Grabaric and J.J. Jackowski, Inorg. Chem., 17 (1978) 2153.
32 F.Y. Pétillon, J.L. Le Quéré, J. Roué, J.E. Guerchais and D.W.A., Sharp, J. Organomet. Chem., 204 (1981) 207 and references therein.
33 J. Courtot-Coupez, J.E. Guerchais, F.Y. Pétillon and J. Talarmin, J. Chem. Soc., Dalton Trans., accepted for publication.
34 G.M. Sheldrick, SHELX 76-78, Program for X-ray structural determinations, University of Cambridge, 1976.